Chemical Science

EDGE ARTICLE

View Article Online
View Journal | View Issue

Cite this: *Chem. Sci.*, 2016, **7**, 1457

Core–shell zeolite@aqueous miscible organic-layered double hydroxides†

Chunping Chen, Coral F. H. Byles, Jean-Charles Buffet, Nicholas H. Rees, Yue Wu and Dermot O'Hare*

Received 27th August 2015
Accepted 13th November 2015

DOI: 10.1039/c5sc03208c

www.rsc.org/chemicalscience

We report a general method for the synthesis of core–shell hybrid materials containing a microporous zeolite core with an aqueous miscible organic-layered double hydroxide (AMO-LDH) shell using a simple *in situ* coprecipitation method. For example, zeolite-HY@AMO-Mg_2Al-CO_3-LDH contains a 150 nm hierarchical AMO-Mg_2Al-CO_3-LDH surface coating on zeolite-HY. It exhibits a similar BET surface area (698 m^2 g^{-1}) as the parent zeolite-HY but this surface area has been re-allocated between microspores and mesopores. We believe that surface aluminium sites act as nucleation sites for the formation of the LDH coating and so robustly links it into the zeolite lattice. We expect that this new hybrid structure with micropores dominating in the core and mesopores populating the shell will provide a desirable new hybrid structure type for adsorption or catalysis.

Introduction

Conventionally, layered double hydroxides (LDHs) are described as anionic clay-like phases possessing a generalised compositional formula $[M^{z+}{}_{1-x}M'^{y+}{}_{x}(OH)_2](X^{n-})_{a/n}\cdot bH_2O$, wherein M and M′ are metal cations, typically $z = 2$ (or 1); $y = 3$ (or 4), $0 < x < 1$, $b = 0$–10, giving $a = z(1 - x) + xy - 2$ and X^{n-} is an organic, bioorganic or inorganic anion.[1–3] They have been widely studied in catalysis,[4,5] adsorption,[6,7] and biomedicine.[8] Typically, LDHs synthesised by conventional methods are hydrophilic, possessing a high water content, and exhibit low surface area and porosity, which impose a limiting scope for their applications. Recently, we have developed a simple and scalable method, the so called aqueous miscible organic solvent treatment (AMOST), to address these issues.[9,10] These LDHs (named AMO-LDHs) possess the generalised formula $[M^{z+}{}_{1-x}M'^{y+}{}_{x}(OH)_2](X^{n-})_{a/n}\cdot bH_2O\cdot c$(AMO-solvent), wherein M and M′ are metal cations, typically $z = 2$ (or 1); $y = 3$ (or 4), $0 < x < 1$, $b = 0$–10, $c = 0.1$–10, (AMO-solvent = an organic solvent 100% miscible with water), $a = z(1 - x) + xy - 2$ and X^{n-} is an organic, bioorganic or inorganic anion. AMO-LDHs are organophilic, exhibiting high surface area with mesoporosity and good dispersibility in non-polar hydrocarbon liquids. AMO-LDHs have already displayed promising applications such as additives to polymers, sorbents and catalyst supports.[9,11–13]

On the other hand, zeolites are a class of crystalline microporous materials, of which the framework is constructed of corner-sharing TO_4 tetrahedral (where T represents a tetrahedrally coordinated Si, Al or a heteroatom).[14,15] Different framework structures lead to very large surface area and high porosity.[15] Such structural versatility and diversity has enabled zeolites to become a material platform of both fundamental and industrial significance.[16–21] However, the typical microporous structure of a zeolite can slow substrate diffusion and/or cause blocking of the active sites in these materials. Recently, new strategies have been introduced to prepare zeolites containing large channels and mesopores, overcoming many of the limitations and drawbacks of mass transfer and diffusion.[14,22,23]

Core–shell structured LDH-based materials have received increasing attention in recent years due to the combination of features from the different materials and the possible synergistic effects between them.[24–27] However, most syntheses are complex and time-consuming. Recently, we developed a facile method to coat AMO-LDH platelets directly onto the surface of spherical silica particles without any pretreatment or binding agents.[28] By adjusting the synthesis conditions, the SiO_2@LDH can be tuned as hollow, yolk-hollow or solid core–shell structures. In this contribution, we have been able to combine the distinguishing properties of both a zeolite and an AMO-LDH by forming core–shell zeolite@AMO-LDH particles with a hierarchical structure.[10,28]

Results and discussion

Particles of zeolite HY(5.1) (5.1 denotes the Si/Al ratio as described in the specification of the commercial product, see ESI†) exhibit a cubic shape morphology with a smooth surface

Chemistry Research Laboratory, Department of Chemistry, University of Oxford, 12 Mansfield Road, Oxford, OX1 3TA, UK. E-mail: dermot.ohare@chem.ox.ac.uk; Tel: +44 (0)1865 272686

† Electronic supplementary information (ESI) available: Experimental details, XRD, HRTEM, FTIR, TGA, BET and ^{29}Si MAS NMR data. See DOI: 10.1039/c5sc03208c

(Fig. S1†). An LDH can be grown from the surface of these cubic crystals by dispersing the zeolite in $NaCO_3$ aqueous solution followed by slow addition of a Mg/Al (2 : 1) nitrate solution at pH = 10. The HY(5.1)@AMO-Mg_2Al-CO_3-LDH was finally isolated by AMOST treatment (AMO solvent = acetone). We find that the LDH platelets grow vertically and randomly on the surface of the zeolite to form a hierarchical layer with the thickness of around 150 nm (Fig. 1A). Energy dispersive X-ray spectroscopy (EDS) mapping (Fig. 1B) reveals that the outer shell is composed of Mg (red) which comes from AMO-Mg_2Al-CO_3-LDH, while the Si (green) from the zeolite is mainly populated in the inner core, indicating that the AMO-Mg_2Al-CO_3-LDH layer has been grown homogenously on the outer shell.

The XRD of HY(5.1)@AMO-Mg_2Al-CO_3-LDH contains both sharp diffraction features from the highly crystalline cubic HY(5.1) core and an additional set of broader Bragg diffraction peaks corresponding to AMO-Mg_2Al-CO_3-LDH, as confirmed by a two-phase Pawley refinement of the XRD data (Fig. 1C, Fig. S2 and Table S1 in ESI†). The FTIR spectrum of HY(5.1)@AMO-Mg_2Al-CO_3-LDH (Fig. S3†) exhibits absorption features from both HY(5.1) and an LDH. In particular, the adsorption band at around 1363 cm^{-1} is associated with a CO_3^{2-} vibration in Mg_2Al-CO_3-LDH. The TGA data for HY(5.1)@AMO-Mg_2Al-CO_3-LDH (Fig. S4†) shows the three thermal events typical of an AMO-LDH. Fig. 1D shows the N_2 adsorption/desorption isotherms for HY(5.1), HY(5.1)@AMO-Mg_2Al-CO_3-LDH, and AMO-Mg_2Al-CO_3-LDH, respectively. The isotherm for HY(5.1) is classically of type I (IUPAC classification),[29] indicating the microporous structure of zeolite.[30] Meanwhile, AMO-Mg_2Al-CO_3-LDH shows a type IV isotherm with H3 type hysteresis loop, indicating that the AMO-Mg_2Al-CO_3-LDH is composed of plate-like particles with slit-shape mesopores.[10,29] The isotherm of the hybrid material shows features of both microporosity and mesoporosity. The pore size distribution obtained from Barrett–Joyner–Halenda (BJH) desorption (Fig. 1D inset) provides more detail on the mesopore distribution. The parent zeolite (HY(5.1)) has a small mesopore distribution at around 3-4 nm while that of AMO-Mg_2Al-CO_3-LDH exhibits a wide range of large mesopores (20–30 nm). We observe that the hybrid HY(5.1)@AMO-Mg_2Al-CO_3-LDH contains both kinds of mesopores. The feature around 3–4 nm increases significantly compared of the initial HY(5.1). Table S2† summarises the specific surface areas. HY(5.1) has a very high N_2 Brunauer–Emmett–Teller (BET) surface area (695 $m^2\ g^{-1}$), most of which is contributed by the micropore surface area (625 $m^2\ g^{-1}$). Pure AMO-Mg_2Al-CO_3-LDH exhibits a N_2 BET surface area of 281 $m^2\ g^{-1}$. Conversely, most of its surface area comes from its external surface area (252 $m^2\ g^{-1}$). After coating the zeolite with an AMO-Mg_2Al-CO_3-LDH layer, the BET surface area (698 $m^2\ g^{-1}$) remains the same as zeolite. However, the allocation of the mesoporosity/microporosity is changed. The external surface area increases dramatically due to the high surface area of AMO-Mg_2Al-CO_3-LDH and/or the generation of new mesopores in zeolite. The micropore surface area decreases to 497 $m^2\ g^{-1}$, which might be due to the coverage of some of the zeolite surface by the LDH. It is worth noting that without applying the AMOST method to the LDH layer, both the external surface area and the micropore surface area of the hybrid are reduced to 95 and 236 $m^2\ g^{-1}$ respectively, indicating that AMO solvent plays a critical role in the formation of a high effective surface area zeolite@LDH core–shell structure. As shown in our previous studies, the AMO solvent can effectively extract the chemisorbed water from the LDH surface and prevent the aggregation with *ab*-face stacking of LDH particles during the drying process.[10] Therefore, LDH without AMO treatment will aggregate as non-porous, stone-like shaped particles, which could block the pores of the zeolite framework.

^{29}Si solid-state nuclear magnetic resonance (NMR) spectroscopic studies of HY(5.1) and HY(5.1)@AMO-Mg_2Al-CO_3-LDH

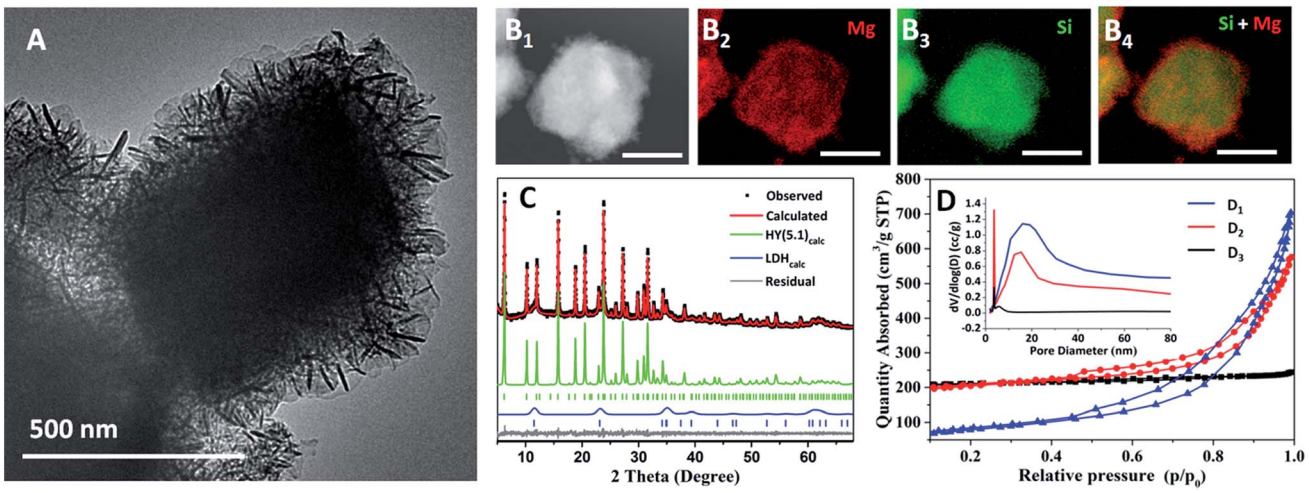

Fig. 1 (A) TEM image of HY(5.1)@AMO-Mg_2Al-CO_3-LDH; (B_1–B_4) STEM and EDX elemental mapping images of HY(5.1)@AMO-Mg_2Al-CO_3-LDH (the scale bars correspond to 500 nm); (C) XRD pattern and two-phase Pawley refinement of HY(5.1)@AMO-Mg_2Al-CO_3-LDH, showing the modelled HY(5.1) and LDH phases; (D) N_2 adsorption/desorption isotherms and pore size distribution (inset) of (D_1) AMO-Mg_2Al-CO_3-LDH, (D_2) HY(5.1)@AMO-Mg_2Al-CO_3-LDH and (D_3) HY(5.1).

were carried out to investigate the silicon environment before and after coating with AMO-Mg_2Al-CO_3-LDH. As shown in Fig. 2A, the HY(5.1) exhibits four characteristic resonances at −92, −97, −103 and −108 ppm, which can be assigned to $Q^4Si(3Al)$, $Q^4Si(2Al)$, $Q^4Si(1Al)$ and $Q^4Si(0Al)$, respectively.[31,32] After coating with a AMO-Mg_2Al-CO_3-LDH layer, HY(5.1)@AMO-Mg_2Al-CO_3-LDH still shows the similar four ^{29}Si NMR resonances at −90, −95, −102 and −108 ppm as shown in Fig. 2B.

However, these resonances were slightly shifted to lower field, probably due to the effect of cation exchange of sodium and/or magnesium with protons during the synthesis of AMO-Mg_2Al-CO_3-LDH.[31,33] In addition, two new NMR features at 113 and 117 ppm were found in the ^{29}Si NMR of the HY(5.1)@AMO-Mg_2Al-CO_3-LDH. These can be assigned to the cristobalite $Q^4(0Al)$, which is due to some lattice degradation by desilication during LDH growth (pH 10 in the AMO-Mg_2Al-CO_3-LDH synthesis process), leading to crystallographic rearrangement.[34,35]

Complying with the principle of Loewenstein's rule (assuming no Al–O–Al linkage in the zeolite framework), the Si/Al ratio in the zeolite framework can be obtained from the Si(*x*Al) peak intensities.[31,33] The data indicate that the Si/Al ratio in the framework of HY(5.1)@AMO-Mg_2Al-CO_3-LDH was around 5.4, lower than the ratio (6.2) in the parent HY(5.1). We believe this is due to the desilication of the zeolite in the alkaline solution. The obtained ratio (6.2) in the parent HY(5.1) is higher than 5.1 as described in the product due to the existence of extra framework aluminium (EFAL). The detailed information for each peak listed in the Table S3† provides consistent evidence. Both resonances for Si(0Al) and Si(1Al) in the framework decreased by around 6–7% while the ones due to Si(2Al) and Si(3Al) increased slightly, which is consistent with the literature.[36,37] Therefore, the Si(0Al) and Si(1Al) could be hydrolysed first under these conditions. In the presence of aluminium, some of the vacancies created by the desilication process will then be re-filled by aluminium which can be either EFAL or the extracted aluminium,[38,39] leading to the slightly more Si(3Al) and Si(2Al) presented in the sample. In our case, EFAL is found in the sample, which can be confirmed by the difference of $(Si/Al)_{bulk}$ (3.78) from EDX and $(Si/Al)_{fw}$ (5.4) from NMR spectroscopy. Furthermore, the ^{27}Al MQ MAS NMR provides additional insights. Beside the main ^{27}Al resonances at around 56 ppm (tetrahedral Al in the zeolite framework), there are another two weak resonances at around 35 and 0 ppm in pure HY(5.1) (Fig. 2C), which are assigned to penta-coordinated and octahedral EFAl species.[40–42] The penta-coordinated Al disappears and the octahedral Al becomes the main peak after coating with the AMO-Mg_2Al-CO_3-LDH layer (Fig. 2D) due to formation of an octahedrally coordinated Al species in the LDH layers. There is another small resonance next to the tetrahedral Al resonance of HY(5.1), which probably arises from the formation of active tetrahedral Al linked to the LDH matrix.

Based on the above discussion, we propose a possible mechanism for the desilication of the zeolite and the formation of AMO-Mg_2Al-CO_3-LDH in HY(5.1)@AMO-Mg_2Al-CO_3-LDH. In the presence of the LDH precursor solution, the highly alkaline conditions lead to the partial desilication of the zeolite, which generates three kinds of structures. As shown in Fig. 3, when desilication occurs in the inside of the framework, it generates mesopores (Fig. 3A) and small vacancies (Fig. 3B) depending on the degree of desilication. The presence of mesopores has been confirmed by the N_2 adsorption/desorption isotherms and the pore size distribution data (Fig. 1D). These vacancies may be re-filled by Al, forming new tetrahedral Si–O–Al linkages in the framework.[38,39] However, when the desilication occurs on the surface of the framework (Fig. 3C), the aluminium inserted in these surface vacancies will be metastable due to the coordination defects.[39] These metastable Al centres could be very active sites for the nucleation of LDH platelet growth on the surface of the zeolite. We observed similar behavior in our previous work on silica@LDH.[28]

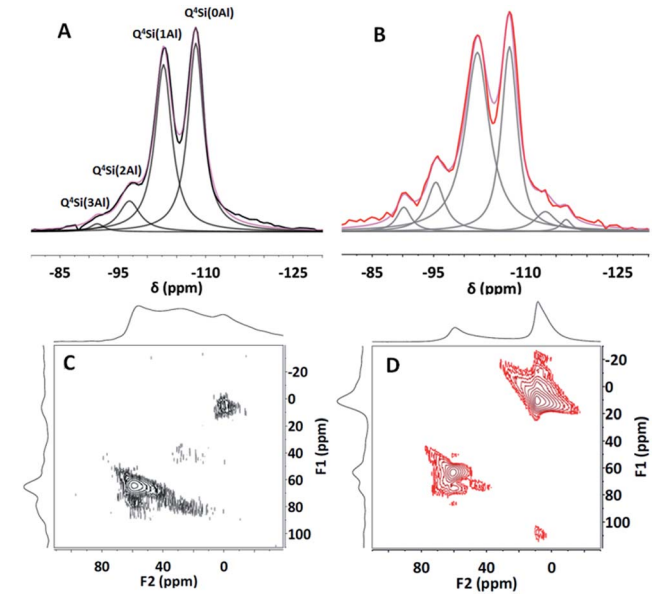

Fig. 2 ^{29}Si solid-state NMR spectra of (A) HY(5.1) and (B) HY(5.1)@AMO-Mg_2Al-CO_3-LDH; ^{27}Al solid-state MQ MAS NMR spectra of (C) HY(5.1) and (D) HY(5.1)@AMO-Mg_2Al-CO_3-LDH.

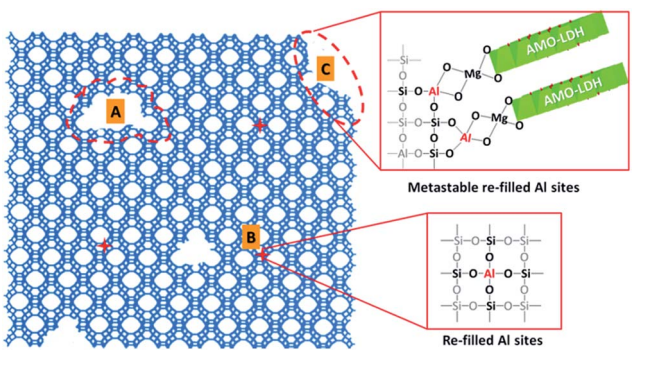

Fig. 3 The proposed mechanism for the desilication of HY(5.1) and the formation of an AMO-Mg_2Al-CO_3-LDH coating on the zeolite surface.

Conclusions

In summary, we have developed a simple method to obtain a core–shell zeolite@AMO-Mg_2Al-CO_3-LDH hybrid material. We find that this simple method is also applicable to other types of zeolite (*e.g.* HY(15) and ZSM5(23)) with either different framework topologies or different Si/Al ratios (Fig. S5†). The AMO-Mg_2Al-CO_3-LDH nanoplatelets can readily grow on the surface of zeolite to form a hierarchical structure without any pre-treatment or binding agent.‡ The obtained HY(5.1)@AMO-Mg_2Al-CO_3-LDH exhibits a similar surface area as the parent zeolite but re-allocates the ratio of micropores and mesopores which can be an effective way to promote mass diffusion and/or exploit new active sites. We found that partial desilication of the HY zeolite has taken place during the synthesis of AMO-Mg_2Al-CO_3-LDH, resulting in the formation of more mesopores and vacancies in the framework. Meanwhile, the re-filled Al on the surface of framework after desilication provides active nucleation sites for the formation of LDH and linking it into the zeolite lattice. We expect that this structure with its micropores dominating in the core and mesopores populating the shell will provide a desirable new hybrid structure type for adsorption or catalysis. The AMO-LDH exterior coating with its mesoporosity and flexible chemical composition should enable the effective tuning of both pore structure and base/acid properties without losing the characteristic properties of the zeolite.

Preliminary catalysis studies using these materials are on going and will be reported shortly. For example, slurry phase polymerisation of ethylene using zeolite@AMO-LDH as a support for metallocene catalysts shows promising synergetic properties between these hybrid materials and polymerisation performance. Solid catalysts based on ZSM-5(23)@AMO-LDH demonstrate around 5 times the activity than the equivalent pristine ZSM-5(23).

Acknowledgements

The authors would like to thank SCG Chemicals Co Ltd, Thailand for funding and YW acknowledges European Union's Seventh Framework Programme (FP7/2007–2013) for funding, grant agreement no. FP7-NMP4-LA-2012-280983, SHYMAN and Dr Alexander Kilpatrick (University of Oxford) for help in BET analysis.

Notes and references

‡ The density and thickness of LDH layer can be affected by the active Si–O–Al surface sites, which can controlled by the Si/Al ratios (Fig. S6†) and the pre-treatment of zeolite (Fig. S7†).

1 X. Duan and D. G. Evans, *Layered double hydroxides,* Springer Verlag, 2006.
2 V. Rives, *layered double hydroxides: present and future*, Nova Science Publishers, 2001.
3 F. Cavani, F. Trifiro and A. Vaccari, *Catal. Today*, 1991, **11**, 173–301.
4 G. Fan, F. Li, D. G. Evans and X. Duan, *Chem. Soc. Rev.*, 2014, **43**, 7040–7066.
5 C. G. Silva, Y. Bouizi, V. Fornés and H. García, *J. Am. Chem. Soc.*, 2009, **131**, 13833–13839.
6 C. Chen, P. Gunawan and R. Xu, *J. Mater. Chem.*, 2011, **21**, 1218–1225.
7 C. Li, M. Wei, D. G. Evans and X. Duan, *Small*, 2014, **10**, 4469–4486.
8 C. Chen, P. Gunawan, X. W. D. Lou and R. Xu, *Adv. Funct. Mater.*, 2012, **22**, 780–787.
9 Q. Wang, X. Zhang, J. Zhu, Z. Guo and D. O'Hare, *Chem. Commun.*, 2012, **48**, 7450–7452.
10 C. Chen, M. Yang, Q. Wang, J.-C. Buffet and D. O'Hare, *J. Mater. Chem. A*, 2014, **2**, 15102–15110.
11 Q. Wang and D. O'Hare, *Chem. Commun.*, 2013, **49**, 6301–6303.
12 (*a*) J.-C. Buffet, N. Wanna, T. A. Q. Arnold, E. K. Gibson, P. P. Wells, Q. Wang, J. Tantirungrotechai and D. O'Hare, *Chem. Mater.*, 2015, **27**, 1495–1501; (*b*) J.-C. Buffet, Z. R. Turner, R. T. Cooper and D. O'Hare, *Polym. Chem.*, 2015, **6**, 2493–2503; (*c*) J.-C. Buffet, T. A. Q. Arnold, Z. R. Turner, P. Angpanitcharoen and D. O'Hare, *RSC Adv.*, 2015, **5**, 87456–87464.
13 M. Yang, O. McDermott, J.-C. Buffet and D. O'Hare, *RSC Adv.*, 2014, **4**, 51676–51682.
14 W. J. Roth, P. Nachtigall, R. E. Morris and J. i. Čejka, *Chem. Rev.*, 2014, **114**, 4807–4837.
15 Y. Li and J. Yu, *Chem. Rev.*, 2014, **114**, 7268–7316.
16 Z. Lai, G. Bonilla, I. Diaz, J. G. Nery, K. Sujaoti, M. A. Amat, E. Kokkoli, O. Terasaki, R. W. Thompson and M. Tsapatsis, *Science*, 2003, **300**, 456–460.
17 I. Kiesow, D. Marczewski, L. Reinhardt, M. Mühlmann, M. Possiwan and W. A. Goedel, *J. Am. Chem. Soc.*, 2013, **135**, 4380–4388.
18 M. Delkash, B. E. Bakhshayesh and H. Kazemian, *Microporous Mesoporous Mater.*, 2015, **214**, 224–241.
19 A. Corma, *Chem. Rev.*, 1997, **97**, 2373–2420.
20 B. Chan and L. Radom, *J. Am. Chem. Soc.*, 2008, **130**, 9790–9799.
21 B. Chan and L. Radom, *J. Am. Chem. Soc.*, 2006, **128**, 5322–5323.
22 J. Perez-Ramirez, C. H. Christensen, K. Egeblad, C. H. Christensen and J. C. Groen, *Chem. Soc. Rev.*, 2008, **37**, 2530–2542.
23 Y. Tao, H. Kanoh, L. Abrams and K. Kaneko, *Chem. Rev.*, 2006, **106**, 896–910.
24 H. Zhang, G. Zhang, X. Bi and X. Chen, *J. Mater. Chem. A*, 2013, **1**, 5934–5942.
25 J. Han, Y. Dou, J. Zhao, M. Wei, D. G. Evans and X. Duan, *Small*, 2013, **9**, 98–106.
26 (*a*) M. Shao, F. Ning, J. Zhao, M. Wei, D. G. Evans and X. Duan, *J. Am. Chem. Soc.*, 2012, **134**, 1071–1077; (*b*) M. Shao, M. Wei, D. G. Evans and X. Duan, *Chem.–Eur. J.*, 2013, **19**, 4100–4108.
27 (*a*) C. Chen, P. Wang, T.-T. Lim, L. Liu, S. Liu and R. Xu, *J. Mater. Chem. A*, 2013, **1**, 3877–3880; (*b*) Z. Gu, J. J. Atherton and Z. P. Xu, *Chem. Commun.*, 2015, **51**, 3024–3036.

28 C. Chen, R. Felton, J.-C. Buffet and D. O'Hare, *Chem. Commun.*, 2015, **51**, 3462–3465.
29 K. Ssing, D. Everett, R. Haul, L. Moscou, R. Pierotti, J. Rouquerol and T. Siemieniewsks, *Pure Appl. Chem.*, 1985, **57**, 603–619.
30 M. Choi, H. S. Cho, R. Srivastava, C. Venkatesan, D.-H. Choi and R. Ryoo, *Nat. Mater.*, 2006, **5**, 718–723.
31 G. Engelhardt and D. Michel, *High-resolution solid-state NMR of silicates and zeolites*, John Wiley and Sons, 1987.
32 E. Lippmaa, M. Mägi, A. Samoson, M. Tarmak and G. Engelhardt, *J. Am. Chem. Soc.*, 1981, **103**, 4992–4996.
33 F. Dogan, K. D. Hammond, G. A. Tompsett, H. Huo, W. C. Conner Jr, S. M. Auerbach and C. P. Grey, *J. Am. Chem. Soc.*, 2009, **131**, 11062–11079.
34 J. Klinowski, *Chem. Rev.*, 1991, **91**, 1459–1479.
35 M. Occelli, A. Schweizer, C. Fild, G. Schwering, H. Eckert and A. Auroux, *J. Catal.*, 2000, **192**, 119–127.
36 D. Serrano and P. Pizarro, *Chem. Soc. Rev.*, 2013, **42**, 4004–4035.
37 A. Fernández-Jiménez, A. Palomo, I. Sobrados and J. Sanz, *Microporous Mesoporous Mater.*, 2006, **91**, 111–119.
38 J. C. Groen, L. A. Peffer, J. A. Moulijn and J. Pérez-Ramírez, *Chem.–Eur. J.*, 2005, **11**, 4983–4994.
39 M.-C. Silaghi, C. Chizallet and P. Raybaud, *Microporous Mesoporous Mater.*, 2014, **191**, 82–96.
40 A. Corma, M. J. Diaz-Cabanas, J. Martínez-Triguero, F. Rey and J. Rius, *Nature*, 2002, **418**, 514–517.
41 T.-H. Chen, K. Houthoofd and P. J. Grobet, *Microporous Mesoporous Mater.*, 2005, **86**, 31–37.
42 C. A. Fyfe, J. L. Bretherton and L. Y. Lam, *J. Am. Chem. Soc.*, 2001, **123**, 5285–5291.